A model for gene therapy of human hereditary lymphedema

Marika J. Karkkainen*, Anne Saaristo*, Lotta Jussila*, Kaisa A. Karila*, Elizabeth C. Lawrence†, Katri Pajusola‡, Hansruedi Bueler‡, Anne Eichmann§, Risto Kauppinen¶, Mikko I. Kettunen¶, Seppo Ylä-Herttuala‖, David N. Finegold†**, Robert E. Ferrell†, and Kari Alitalo*††

*Molecular/Cancer Biology Laboratory and Ludwig Institute for Cancer Research, Haartman Institute and Helsinki University Hospital, Biomedicum Helsinki, University of Helsinki, P.O.B. 63 (Haartmaninkatu 8), 00014 Helsinki, Finland; †Department of Human Genetics, University of Pittsburgh, 130 DeSoto Street, Pittsburgh, PA 15261; ‡Institute of Molecular Biology, University of Zürich, Winterthurerstrasse 190, 8057 Zürich, Switzerland; §Institut d'Embryologie Cellulaire et Moléculaire du Centre National de la Recherche Scientifique et du Collège de France 49bis, Avenue de la Belle Gabrielle, 94736 Nogent-sur-Marne Cedex, France; ¶National Bio-Nuclear Magnetic Resonance Facility and ‖Department of Medicine, A.I. Virtanen Institute, University of Kuopio, P.O.B. 1627, 70211 Kuopio, Finland; and **Department of Pediatrics, University of Pittsburgh, 3705 Fifth Avenue, Pittsburgh, PA 15213

Primary human lymphedema (Milroy's disease), characterized by a chronic and disfiguring swelling of the extremities, is associated with heterozygous inactivating missense mutations of the gene encoding vascular endothelial growth factor C/D receptor (VEGFR-3). Here, we describe a mouse model and a possible treatment for primary lymphedema. Like the human patients, the lymphedema (Chy) mice have an inactivating *Vegfr3* mutation in their germ line, and swelling of the limbs because of hypoplastic cutaneous, but not visceral, lymphatic vessels. Neuropilin (NRP)-2 bound VEGF-C and was expressed in the visceral, but not in the cutaneous, lymphatic endothelia, suggesting that it may participate in the pathogenesis of lymphedema. By using virus-mediated VEGF-C gene therapy, we were able to generate functional lymphatic vessels in the lymphedema mice. Our results suggest that growth factor gene therapy is applicable to human lymphedema and provide a paradigm for other diseases associated with mutant receptors.

Hereditary or primary lymphedema (Milroy's disease) is a developmental disorder, in which defective cutaneous lymphatic vessels fail to transport lymphatic fluid, resulting in swelling of the extremities. Primary lymphedema is inherited as an autosomal dominant trait with reduced penetrance, variable expression, and variable age at onset (1). Several groups have reported linkage of lymphedema to chromosome 5q (2–4), and we have shown that mutant, inactive vascular endothelial growth factor receptor-3 (VEGFR-3) tyrosine kinase is responsible for lymphedema in several such families (5, 6). Recently, it has also been suggested that lymphedema in patients having ectodermal dysplasia with immunodeficiency may be caused by defective VEGFR-3 signaling via the nuclear factor (NF)-κB transcription factor (7).

VEGFR3 is one of the rare genes expressed almost exclusively in the lymphatic endothelial cells in adults (8, 9), although it is also needed for proper generation of the embryonic blood vasculature (10). Overexpression of the VEGFR-3 ligands VEGF-C and VEGF-D in the skin of transgenic mice induced the formation of a hyperplastic lymphatic vessel network (11, 12). Similar results were obtained by using the C156S mutant form of VEGF-C (12, 13), which is specific for VEGFR-3, indicating that lymphatic growth is regulated via this receptor. In addition, expression of ligand-blocking concentrations of soluble VEGFR-3 in transgenic mice inhibited the development of the lymphatic vasculature in several organs (14).

Here, we have analyzed the Chy mutant mice that develop chylous ascites after birth (15, 16). We show that, like the human lymphedema patients, these mice have a heterozygous inactivating *Vegfr3* mutation and swelling of the limbs because of a lack of s.c. lymphatic vessels. By using viral gene delivery and transgenic approaches, we have explored the possible therapeu-

tic effect of VEGF-C in the Chy mice. We show that VEGFR-3 ligand overexpression induces the growth of functional cutaneous lymphatic vessels in the Chy mice, suggesting that VEGF-C/D therapy is applicable also to human lymphedema.

Materials and Methods

Mouse Lines. The Chy phenotype was found among the offspring of a male C3H mouse treated with 250 mg/kg ethylnitrosourea, in the Medical Research Council Mammalian Genetics Unit Embryo Bank (Harwell, U.K.). To identify the *Vegfr3* intron/exon boundaries, we aligned the *Vegfr3* cDNA sequence (Accession no. L07296) with the *VEGFR3* genomic sequence (17), and amplified exons 16 through 26 of *Vegfr3*, which were then sequenced from the C3H, B6, BALB/c, BbxD2, and PES strains. We used the K14-VEGF-C156S and *Vegfr3*$^{+/-}$ mice in the crosses (10, 12).

***In Vitro* Studies of the Mutant Receptor.** We generated the human VEGFR-3(I1053F) expression vector (Accession nos. X68203 and S66407) by using the GeneEditor *in vitro* Site-Directed Mutagenesis kit (Promega), and the oligonucleotide 5′-CATAGTGAAGTTCTGCGACTT-3′, followed by construct transfection into 293T cells, immunoprecipitation, and Western blotting, as previously described (5).

Analyses of Lymphatic and Blood Vessels. To visualize the lymphatic network in the ear, we followed the staining of the lymphatic vessels by fluorescence microscopy after intradermal injection of FITC-dextran (Sigma). For analysis of the deeper lymphatic vessel function, we injected Evans blue (Sigma, 3 mg/ml in PBS) intradermally into the hind footpads. The skin of the limb was then removed to expose the region of the ischiatic vein. To visualize the blood vessels in whole-mount tissue preparations, we used biotinylated *Lycopersicon esculentum* lectin, as previously described (12, 18).

Immunohistochemistry (IHC). We fixed tissue biopsies in 4% paraformaldehyde, dehydrated them, and embedded them in paraffin. We stained 5-μm sections with antibodies against VEGFR-3 (19), lymphatic vessel endothelial hyaluronan receptor-1

(LYVE-1; ref. 20), podoplanin (21), platelet endothelial cell adhesion molecule-1 (PECAM-1) (PharMingen), or hVEGF-C (22), by using a Tyramide Signal Amplification kit (TSA, NEN). We developed the peroxidase activity with 3-amino-9-ethyl carbazole (Sigma), and counterstained the sections with hematoxylin. We used the biotinylated anti-mouse VEGFR-3 Ab (R&D Systems, Oxon, U.K.) for whole-mount stainings.

Magnetic Resonance Imaging (MRI). For high resolution MRI of the feet, mice (Chy, $n = 2$; and wild-type (WT), $n = 2$) were anesthetized and externally fixed to a custom-built animal holder. Animals were kept normothermic by blowing warm air to the magnet bore. MRI data were acquired by using a s.m.i.s. console (Surrey Medical Imaging Systems, Guildford, U.K.) interfaced to a 9.4 T vertical magnet (Oxford Instruments, Oxford, U.K.). A single loop surface coil (diameter 35 mm) was used for signal transmission and detection. A T_2-weighted [repetition time (TR) 2000 ms, echotime (TE) 40 ms, eight scans perline] multislice spin-echo sequence was used with a field of view of 25.6×12.8 mm^2 (matrix size 256×64) and slice thickness of 1.3 mm in transverse orientation. Diffusion weighted MRI was acquired by using monopolar diffusion gradients (b values 330 and 700 s/mm^2) along slice axis in the spin-echo sequence (TR 2000 ms, TE 35 ms), and water apparent diffusion coefficient was computed by fitting the MRI data as function of b-values into a single exponential.

VEGF-C Binding Assays. We assembled the human neuropilin (hNRP)-2(a22) cDNA encoding the extracellular domain (23) from Integrated Molecular Analysis of Genomes and their Expression (IMAGE) Consortium cDNA clones (Incyte Genomics, St. Louis, MO) and cloned it into the pIgplus vector (Ingenius, R&D Systems) in frame with the human IgG1 Fc tail. For receptor-IgG production, we transfected the expression vectors encoding NRP-2-IgG or VEGFR-3-IgG (14) into 293T cells. After 30 h, the cells were starved for 24 h in a medium containing 0.2% BSA, and the medium was used for the binding assays. For growth factor production, we transfected 293EBNA cells with expression vectors encoding human full-length VEGF-C or VEGF, or an empty vector, labeled the cells with 100 μCi/ml [^{35}S]Met/[^{35}S]Cys (Promix, Amersham) for 15 h and immunoprecipitated the media from the VEGF-C and vector-transfected cells with VEGF antibodies (R&D Systems) for depletion of endogenous VEGF. The binding assay was performed as described previously (12). For adeno-associated virus (AAV)-VEGF-C binding assay, we infected ca. 3.5×10^6 HeLa cells with 8×10^{10} particles of AAV-VEGF-C or AAV-EGFP viruses for 8 h in medium containing 2% FCS, glutamine, and antibiotics. After 3 days, the cells were labeled, and the medium was VEGF immunoprecipitated and subjected to binding assays or immunoprecipitation with VEGF-C antibodies.

Production of AAVs Encoding VEGF-C. We cloned the complete coding region of VEGF-C (22) as a blunt-end fragment into the *Mlu*I site of psub-CMV-WPRE (24). We cotransfected 293T cells with recombinant rAAV vector plasmid, AAV packaging plasmid pAAV/Ad-rep(ACG), and adenovirus helper plasmid pBS-E2A-VA-E4 (24). Sixteen hours later, we replaced the medium by fresh complete growth medium. We collected the cells 48 h after transfection, and released rAAVs by four freeze-thaw cycles in liquid nitrogen. We purified the rAAV by an Iodixanol-gradient ultracentrifugation and heparin-Sepharose HPLC (25).

Viral VEGF-C Overexpression. An amount equal to 2–5×10^8 plaque-forming units of the adenoviruses encoding VEGF-C or LacZ, or 5×10^9–1×10^{11} rAAV particles encoding VEGF-C or EGFP were injected intradermally into the right ear, the left
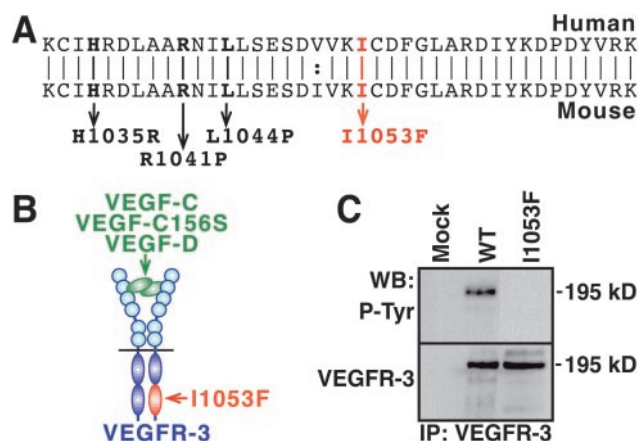

Fig. 1. The VEGFR-3(I1053F) mutant is tyrosine kinase inactive. (*A*) The alignment of the human and mouse VEGFR-3 amino acid sequences showing the lymphedema-linked human mutations (bold) and the I1053F mutation found in the Chy mice (red). (*B*) Localization of the I1053F mutation within the catalytic domain of the ligand-bound VEGFR-3 heterodimer. (*C*) VEGFR-3(I1053F) is kinase inactive. We transfected cells with Mock, WT, or I1053F VEGFR-3 expression vectors and analyzed VEGFR-3 by immunoprecipitation and Western blotting of the cell lysates using phosphotyrosine antibodies (*Upper*). We also confirmed the expression of similar amounts of VEGFR-3 (*Lower*).

ear serving as a negative control. We killed the mice 2 weeks after adenoviral or 3 to 7 weeks after AAV gene transfer and confirmed the adenoviral protein expression in the ear by 5-bromo-4-chloro-3-indolyl β-D-galactoside (X-Gal) staining for β-galactosidase activity, and the AAV-EGFP expression by fluorescent microscopy.

Northern Blotting. We extracted total RNA by using the RNeasy kit (Qiagen, Chatsworth, CA) and electrophoresed 10 μg of RNAs in 1% agarose, followed by transfer to nylon filters (Nytran, Schleicher & Schuell), hybridization with ^{32}P-labeled cDNA probes, and exposure in autoradiography.

Results

A Mouse Model for Primary Lymphedema. A Chy mouse mutant, characterized by the accumulation of chylous ascites into the abdomen, and swelling of the limbs, was originally obtained by ethylnitrosourea-induced mutagenesis (15, 16). This phenotype was linked to mouse chromosome 11. We sequenced the *Vegfr3* candidate gene of this chromosome in the Chy mice and found a heterozygous A3157T mutation resulting in I1053F substitution in the tyrosine kinase domain (Fig. 1 *A* and *B*). This mutation is located in a highly conserved catalytic domain of the receptor, in close proximity to the VEGFR-3 mutations in human primary lymphedema (5, 6). We did not detect this mutation in the parental C3H mouse strain, or in the other strains analyzed.

VEGFR-3(I1053F) Mutant Receptor Is Tyrosine Kinase Inactive. To analyze how the I1053F substitution affects VEGFR-3 phosphorylation, we expressed the corresponding mutant human VEGFR-3 transiently in conditions where its overexpression results in ligand-independent phosphorylation. Unlike for the WT receptor, we detected no phosphorylation of VEGFR-3(I1053F) (Fig. 1C). This finding is consistent with the results obtained with the mutant tyrosine kinase-inactive VEGFR-3s in human primary lymphedema. When we mated the Chy mice with the *Vegfr3*$^{+/-}$ mice, in which one *Vegfr3* allele is disrupted by the *LacZ* sequence (10), no offspring carrying both mutations were born. At embryonic day (E) 10.5, such embryos were growth
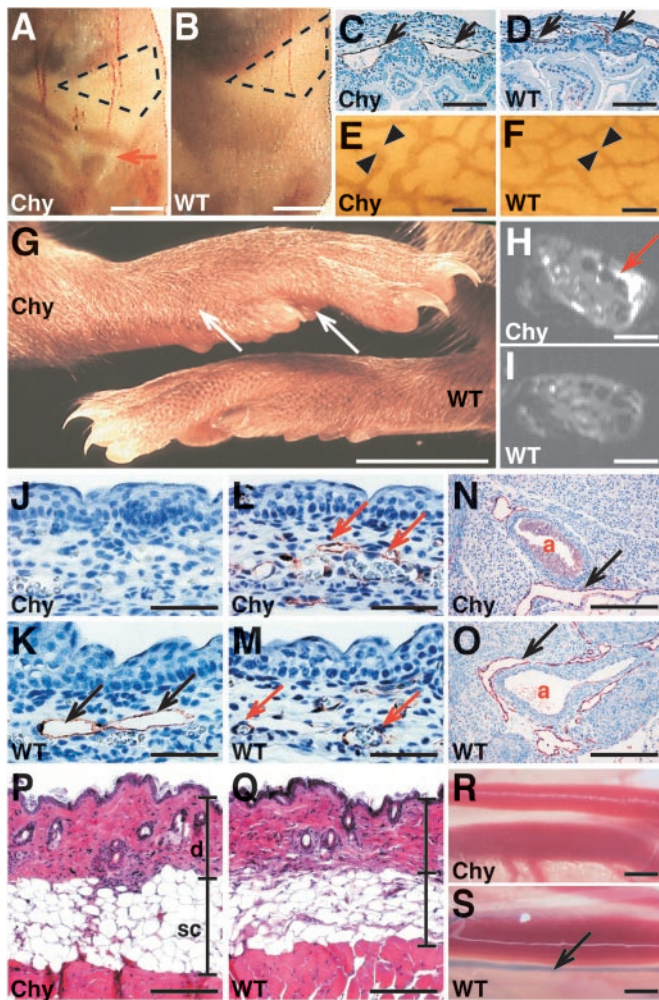
Fig. 2. Defective lymphatic vessels in the Chy mice. (*A* and *B*) The Chy mice were recognized by the accumulation of chyous fluid into the abdomen (red arrow). WT littermate is shown as a comparison. The stomach is marked with a dashed line. (*C–F*) The subserosal lymphatic vessels are enlarged in the Chy mouse intestine as detected by VEGFR-3 IHC (*C* and *D*), and by VEGFR-3 wholemount staining (*E* and *F*). (*G*) The feet of the Chy mice are swollen (arrows), when compared with a WT littermate. (*H* and *I*) MRI of the mouse feet shows the prominent hyperintensity in the Chy mouse foot, which is absent in a WT mouse. (*J* and *K*) The lymphatic endothelium (black arrows) of E15.5 skin was visualized by VEGFR-3 IHC in the Chy and WT mice. Note the absence of the lymphatic vessels in the Chy mice. (*L* and *M*) PECAM-1 IHC reveals no differences in the blood vasculature (red arrows). (*N* and *O*) VEGFR-3 IHC indicates that the lymphatics surrounding the aorta (a) in the Chy mice are similar to those of the WT mice. (*P* and *Q*) The hematoxylin-eosin staining of the back skin shows that the dermis (d) and s.c. adipose tissue (sc) are thickened in the Chy mice when compared with the WT littermate. (*R* and *S*) The transport of the Evans blue dye into the collecting lymphatic vessels (arrow) was visualized in the WT but not in the Chy mice after intradermal injection of the dye. [Bars = 5 mm (*A* and *B*), 90 μm (*C* and *D*), 200 μm (*E* and *F*), 5 mm (*G*), 100 μm (*H* and *I*), 70 μm (*J–M*), 200 μm (*N* and *O*), 210 μm (*P* and *Q*), and 1.5 mm (*R* and *S*).]

retarded, suggesting that they die approximately at the same developmental stage as the *Vegfr3*$^{-/-}$ mice. These results support the idea that there is no signaling via the VEGFR-3(I1053F).

The Chy Mice Have Defective Lymphatic Vessels. The Chy phenotype was characterized by the appearance of chylous fluid in the abdomen (Fig. 2 *A* and *B*). Approximately 10% of the affected pups developed a severe fluid accumulation during the three first postnatal weeks. This condition was associated with histopatho-

logical changes in the liver, fibrinous adhesions of the intestinal tract, and lethality. The chylous fluid was spontaneously resorbed from the rest of the mice, which then appeared healthy, developed normally, and were fertile. IHC for the lymphatic endothelial markers showed that their lymphatic vessels were enlarged in the intestinal subserosal tissue (Fig. 2 *C–F*). These results are consistent with similar findings in human lymphedema (26, 27).

Primary lymphedema is characterized by chronic, disfiguring swelling of one or several limbs. The chronic lymphatic dysfunction leads to thickening of the skin, accumulation of adipose tissue, and dermal fibrosis of the affected areas (28). The feet of the Chy mice are swollen, indicating possible defects in the lymphatic vessels (Fig. 2*G*). MRI of the feet revealed prominent T$_2$-hyperintense regions in s.c. tissues of the Chy mice (Fig. 2*H*), but not in WT mice (Fig. 2*I*). The apparent diffusion coefficient (ADC) of these hyperintense areas was $(2.34 \pm 0.30) \times 10^{-3}$ mm^2/s, about 70% of ADC of free water at 37°C, which was higher than in normal appearing tissue [ADC $(1.54 \pm 0.09) \times 10^{-3}$ mm^2/s]. The observed high diffusion coefficient suggests that hyperintense regions contain elevated amounts of fluid.

IHC for the lymphatic endothelial markers VEGFR-3, lymphatic vessel endothelial hyaluronan receptor-1 (LYVE-1; ref. 20), and podoplanin (21) revealed lack of lymphatic vessels in the Chy mouse skin, when compared with the WT littermate (Fig. 2 *J* and *K*; and data not shown). However, we observed few enlarged cutaneous lymphatic vessels in the Chy mice, consistent with similar findings in human hereditary lymphedema. We did not detect changes in the blood vessels stained for the platelet endothelial cell adhesion molecule-1 (PECAM-1) (Fig. 2 *L* and *M*), or when analyzed by biotin-labeled *L. esculentum* lectin perfusion (ref. 18 and data not shown). Also, the larger collecting lymphatic vessels and VEGFR-3-positive fenestrated blood vessels appeared normal in the Chy mice (ref. 9; Fig. 2 *N* and *O*; and data not shown). In histological examination, the dermis and s.c. adipose tissue were thickened in the Chy mice, when compared with the WT littermates (Fig. 2 *P* and *Q*). We also analyzed lymphatic fluid transport by intradermal injection of the Evans blue dye into the hind footpads, and by observing the appearance of the dye in the deeper collecting lymphatic vessels. We detected no transport of the dye in the Chy mice (Fig. 2*R*), whereas the lymphatic vessels alongside of the ischiatic vein were rapidly stained in the WT mice (Fig. 2*S*).

Dermal Lymphatic Vessels Lack the VEGF-C Binding Protein NRP-2. One possibility to explain the lack of lymphatic hypoplasia in the visceral organs of the Chy mice is that VEGF-C interacts with a second receptor in these organs. NRP-1 and NRP-2 are transmembrane receptors that are required for axon guidance, and they bind semaphorins as well as certain VEGF family members (29–31). To analyze whether VEGF-C binds NRP-2, we tested the ability of a soluble human NRP-2/IgG1 Fc fusion protein to interact with VEGF-C (Fig. 3*A*). We detected binding of VEGF-C to NRP-2, and, unlike for VEGF (30), this binding was not affected by heparin (data not shown). Surprisingly, in IHC we obtained a strong NRP-2 signal from the intestinal lymphatic endothelium, but not from the blood vessels (Fig. 3 *B* and *C*). In contrast, we did not detect NRP-2 staining in the lymphatic vessels of the skin (Fig. 3 *D* and *E*). These results suggest that there is a difference in VEGF-C receptor expression between the affected and unaffected lymphatic vessels.

Gene Therapy for Lymphedema via Adenoviral VEGF-C Expression. Because the molecular mechanisms leading to the hereditary lymphedema phenotypes are only beginning to be resolved, there is no biologically based treatment for this disease. We wanted to know whether we could stimulate lymphatic growth in the Chy mice by VEGFR-3 ligand administration via an adenovirus
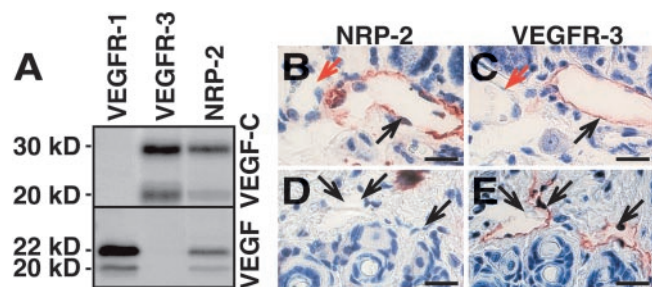
Fig. 3. NRP-2 binds VEGF-C and is differentially expressed in the visceral organs and in the skin. (*A*) Labeled VEGF-C is precipitated by VEGFR-3-IgG and by NRP-2-IgG, but not by VEGFR-1-IgG fusion protein. (*B* and *C*) The intestinal VEGFR-3-positive lymphatic vessels (*C*; black arrow) stain also for NRP-2 (*B*), whereas the blood vessels are not stained (red arrows). (*D* and *E*) The VEGFR-3-positive vessels in the skin (*E*) are not stained by the NRP-2 antibodies (*D*). (Bars = 35 μm.)
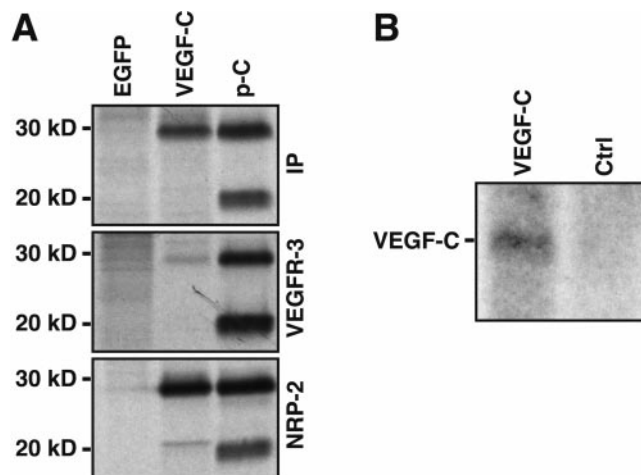

Fig. 4. Analysis of the AAV-VEGF-C expression. (*A*) AAV-produced VEGF-C polypeptides were metabolically labeled and subjected to immunoprecipitation with VEGF-C antibodies (IP) or to binding assay with soluble VEGFR-3 and NRP-2 IgG fusion proteins. AAV-EGFP-infected cells were used as a negative control and VEGF-C produced in 293T cells as a positive control (p-C). (*B*) Northern blotting of total RNA from AAV-VEGF-C-infected and control ears of a Chy mouse.

encoding VEGF-C (AdVEGF-C; refs. 32 and 33). We infected the ears of the Chy mice by intradermal injection of AdVEGF-C or control virus encoding β-galactosidase (AdLacZ; ref. 34). After 2 weeks, we detected functional lymphatic vessels in the AdVEGF-C-infected ears, as shown by the uptake of FITC-dextran injected intradermally into the ears (see Fig. 5*A*). We also confirmed the presence of the lymphatic vessels by IHC (see Fig. 5*B*). We also confirmed the presence of the lymphatic vessels on by IHC (see Fig. 5*B*). AdLacZ-infected Chy ears had strong β-galactosidase expression but no transport of FITC-dextran (data not shown). These results show that a lymphangiogenic response is obtained by adenoviral VEGF-C gene transfer in the Chy mice.

VEGF-C Gene Therapy via AAV. Although we were able to stimulate growth of functional lymphatic vessels by adenoviral VEGF-C expression, no long-term expression could be obtained by using this virus because of a strong immune response against it. Like the adenoviruses, AAV infects both dividing and quiescent cells of several organs, but it gives long-term transgene expression without cell-mediated immune response or toxicity (35). We constructed a rAAV expression vector for VEGF-C, and used AAV encoding enhanced green fluorescent protein (EGFP) as a control (24). We confirmed the AAV-mediated VEGF-C production from rAAV-infected, metabolically labeled HeLa cell culture media by immunoprecipitation and gel electrophoresis. We detected production of the major 30-kDa form of VEGF-C, but very little or no 20-kDa form (Fig. 4*A*). We also confirmed the binding of AAV-produced VEGF-C to its receptors by using the soluble receptor-IgG fusion proteins. In this binding assay, we detected binding of the major 30-kDa form of VEGF-C to VEGFR-3 and to NRP-2 (Fig. 4*A*).

To analyze the *in vivo* effects of AAV-mediated VEGF-C expression, we infected mouse ears by intradermal injection, and analyzed the effects after 3 to 7 weeks. We confirmed VEGF-C RNA expression in the infected ears (Fig. 4*B*), and in parallel, detected AAV-EGFP expression in fluorescence microscopy (data not shown). In the fluorescent microlymphography, we detected functional lymphatic vessels in the AAV-VEGF-C-infected Chy ears, but not in the control ears (Fig. 5 *C* and *D*). The formation of lymphatic vessels in the AAV-VEGF-C-infected Chy mouse ears was confirmed by IHC analysis (Fig. 5 *E* and *F*). Furthermore, the dye was transported into the collecting lymphatic vessels in the AAV-VEGF-C-treated but not untreated Chy ears (Fig. 5 *G* and *H*). In the WT mice, AAV-VEGF-C expression did not affect the lymphatic vessel function (Fig. 5 *I–L*), although in some cases we observed a

denser lymphatic network, resembling that in the transgenic mice overexpressing VEGFR-3 ligands in the skin (11, 12).

Lymphatic Vessel Growth Stimulated by a VEGFR-3-Specific Ligand. VEGF-C is also capable of binding to VEGFR-2, and it may thus affect blood vessels. We therefore analyzed whether a VEGFR-3-specific growth factor can induce lymphatic growth in the Chy model. We mated the Chy mice with mice expressing VEGF-C156S in the skin keratinocytes (12). In these mice, transgene expression begins between E14.5 and E16.5, and thus there is no immune response toward the encoded proteins (36). IHC revealed the presence of lymphatic vessels in the skin of the Chy × K14-VEGF-C156S mice (Fig. 6 *A–C*), whereas the blood vessels were not affected (Fig. 6 *D–F*). The VEGF-C156S transgene expression was detected in the hair follicles by IHC (Fig. 6 *G–I*). FITC-dextran microlymphography of the ears showed that a WT-like lymphatic function was restored in the Chy × K14-VEGF-C156S mice (Fig. 6 *J–L*). These results indicate that VEGFR-3 stimulation with an excess of its specific ligand is sufficient to overcome the lymphatic hypoplasia caused by the mutant receptor allele.

Discussion

The molecular mechanisms and environmental factors affecting the pathogenesis and variable age of onset of lymphedema are largely unclear (28). In human patients, fluorescence microlymphography or lymphoscintigraphy reveal lack of a functional lymphatic vessel network at sites of edema. This finding is consistent with the hypoplasia of the cutaneous lymphatic vessels in the Chy mice. Currently, lymphedema is treated by manual lymphatic drainage and by compressive garments. The discovery of specific genes involved in the pathogenesis of lymphedema now allows us to study more targeted therapies for this disease.

Although the lymphedema patients with heterozygous missense mutations of *VEGFR3* retain some receptor activity because of the presence of the WT allele (5), the mutant VEGFR-3 can be classified as a dominant negative receptor similar to certain mutant KIT receptors in piebaldism and rearranged during transportation (RET) receptors in Hirschprung's disease (5, 37). It has been unclear whether ligand therapy could be effective for the treatment of such diseases.

Fig. 5. Gene therapy by using viral VEGF-C overexpression. (*A* and *B*) Adenovirally induced VEGF-C overexpression in a Chy mouse ear induces formation of functional lymphatic vessels, as analyzed by fluorescent microlymphography (*A*) or by VEGFR-3 IHC (*B*). The dye depot is marked with a dashed line. (*C* and *D*) Microlymphography of the lymphatic vessels 7 weeks after AAV infection reveals functional lymphatic vessels (white arrows) in the AAV-VEGF-C-infected Chy ear (*C*) when compared with the control ear (*D*). (*E* and *F*) VEGFR-3 IHC shows that the AAV-VEGF-C-infected Chy ears contain VEGFR-3-positive vessels (*E*, black arrows), whereas no staining is detected in the AAV-EGFP-infected ears (*F*). (*G* and *H*) The fluorescent dextran was collected by the draining lymphatic vessel (white arrow) in the AAV-VEGF-C-treated Chy ear (*G*), unlike in the noninfected ear of the same mouse (*H*). Red arrows mark the blood vessels, and an arrowhead marks the cartilage of the ear. (*I* and *J*) In WT mice, there are no major changes in lymphatic vasculature after AAV-VEGF-C infection (*I*), when compared with the control ears (*J*). (*K* and *L*) The same is also confirmed by VEGFR-3 IHC. [Bars = 200 μm (*A*), 150 μm (*B*, *E*, *F*, *K*, and *L*), 300 μm (*C*, *D*, *I*, and *J*), and 5 mm (*G* and *H*).]

Here, by treating the Chy mice with viral VEGF-C gene therapy, we were able to induce the growth of functional lymphatic vessels in their skin. Milroy's disease would thus provide one example of a human hereditary disease where gene therapy seems feasible, and it could provide a paradigm for other diseases associated with mutant receptors.

Fig. 6. Lymphatic vessel growth in the Chy × K14-VEGF-C156S mice. (*A–C*) Staining by using VEGFR-3 antibodies shows lymphatic vessels (black arrows) in the ear of the Chy × K14-VEGF-C156S mice, in comparison with the aplastic lymphatic vessels in the Chy mouse ear (*B*), or with the WT littermate (*C*). (*D–F*) PECAM IHC confirms that the blood vasculature is normal in all mice. (*G–I*) VEGF-C IHC shows the VEGF-C156S transgene expression in the basal cells of the hair follicles (red arrows). (*J–L*) Fluorescent microlymphography shows the functional lymphatic capillary network in the Chy × K14-VEGF-C156S ear (*J*), resembling that of the WT mouse (*L*). The FITC-dextran is not collected into the lymphatic vessels in the Chy mouse ear (*K*). [Bars = 70 μm (*A–F*), 25 μm (*G–I*), and 600 μm (*J–L*).]

In the skin, VEGF-D is expressed in the close proximity to the superficial lymphatic vessel network (38) and may be regulated by cell–cell contacts in the dermis (39), whereas VEGF-C is only weakly expressed. However, we did not detect major differences in the VEGF-C or VEGF-D levels between the Chy and WT mice. Our present results, along with those of Mäkinen *et al.* (14) support the idea that the cutaneous lymphatic vessels are regulated differently from those in other organs, and that besides VEGF-C and VEGF-D, there are additional signals for growth and maturation of the lymphatic endothelium. We show here that NRP-2 binds VEGF-C, and is expressed in the lymphatic vessels of internal organs, but not in the skin. Therefore, it is possible that NRP-2 is involved in the VEGFR-3-mediated signal transduction at sites where the two receptors are coexpressed, similar to what has been reported for NRP-1 regulation of VEGFR-2-mediated angiogenic signals (29). Expression only in a subset of lymphatic vessels has also been described for the β-chemokine receptor D6, reflecting the heterogeneity of the different types of lymphatic vessels (40).

Our results with the Chy mouse model suggest that overexpression of VEGFR-3 ligands could be used also in patients via viral or plasmid vector transfer, or via protein administration into the affected tissues. Such therapy could be even more effective in non-hereditary, more regional forms of lymphedema, resulting from traumas, surgery, or lymphatic vessel destruction e.g., after filarial infection. Because VEGF-C also binds VEGFR-2 on blood vascular endothelium, it is capable of

stimulating vascular permeability and, in some conditions, angiogenesis (22, 41). Because of possible complications due to tissue edema or accelerated tumor angiogenesis, the VEGFR-3-specific growth factor VEGF-C156S could thus be a more attractive choice for therapeutic applications. An additional concern would be the fact that tumor lymphangiogenesis has been associated with enhanced lymph node metastasis (42). Thus, treatment of lymphedema arising in the arm after axillary lymphadenectomy in association with breast cancer surgery may pose a problem, because it could enhance the growth and spread of dormant metastases. However, the half-life of VEGF-C in the blood circulation is short (12), and local VEGF-C therapy is thus likely to function without systemic effects.

In conclusion, we have analyzed here a mouse model for Milroy's disease with swelling of the limbs because of a hypoplastic s.c. lymphatic network. Like certain lymphedema patients, the Chy mice carry a heterozygous inactivating *Vegfr3* mutation. The pathogenesis of lymphedema, and its consequences, such as fat deposition, fibrosis, and compromised immune function can now be analyzed by using the Chy mice. By overexpressing VEGF-C in the skin, we obtained growth of functional cutaneous lymphatic vessels in the Chy mice. This result suggests that the VEGF-C administration alone or in combination with other lymphangiogenic factors could be a powerful tool in the therapy of various forms of human lymphedema.

1. Witte, M. H., Way, D. L., Witte, C. L. & Bernas, M. (1997) in *Regulation of Angiogenesis*, eds. Goldberg, I. D. & Rosen, E. M. (Birkhäuser, Basel), pp. 65–112.
2. Ferrell, R. E., Levinson, K. L., Esman, J. H., Kimak, M. A., Lawrence, E. C., Barmada, M. M. & Finegold, D. N. (1998) *Hum. Mol. Genet.* **7,** 2073–2078.
3. Witte, M. H., Erickson, R., Bernas, M., Andrade, M., Reiser, F., Conlon, W., Hoyme, H. E. & Witte, C. L. (1998) *Lymphology* **31,** 145–155.
4. Evans, A. L., Brice, G., Sotirova, V., Mortimer, P., Beninson, J., Burnand, K., Rosbotham, J., Child, A. & Sarfarazi, M. (1999) *Am. J. Hum. Genet.* **64,** 547–555.
5. Karkkainen, M. J., Ferrell, R. E., Lawrence, E. C., Kimak, M. A., Levinson, K. L., McTigue, M. A., Alitalo, K. & Finegold, D. N. (2000) *Nat. Genet.* **25,** 153–159.
6. Irrthum, A., Karkkainen, M. J., Devriendt, K., Alitalo, K. & Vikkula, M. (2000) *Am. J. Hum. Genet.* **67,** 295–301.
7. Döffinger, R., Smahi, A., Bessia, C., Geissmann, F., Feinberg, J., Durandy, A., Bodemer, C., Kenwrick, S., Dupuis-Girod, S., Blanche, S., *et al.* (2001) *Nat. Genet.* **27,** 277–285.
8. Kaipainen, A., Korhonen, J., Mustonen, T., van Hinsbergh, V. W. M., Fang, G.-H., Dumont, D., Breitman, M. & Alitalo, K. (1995) *Proc. Natl. Acad. Sci. USA* **92,** 3566–3570.
9. Partanen, T. A., Arola, J., Saaristo, A., Jussila, L., Ora, A., Miettinen, M., Stacker, S. A., Achen, M. G. & Alitalo, K. (2000) *FASEB J.* **14,** 2087–2096.
10. Dumont, D. J., Jussila, L., Taipale, J., Lymboussaki, A., Mustonen, T., Pajusola, K., Breitman, M. & Alitalo, K. (1998) *Science* **282,** 946–949.
11. Jeltsch, M., Kaipainen, A., Joukov, V., Meng, X., Lakso, M., Rauvala, H., Swartz, M., Fukumura, D., Jain, R. K. & Alitalo, K. (1997) *Science* **276,** 1423–1425.
12. Veikkola, T., Jussila, L., Makinen, T., Karpanen, T., Jeltsch, M., Petrova, T. V., Kubo, H., Thurston, G., McDonald, D. M., Achen, M. G., *et al.* (2001) *EMBO J.* **6,** 1223–1231.
13. Joukov, V., Kumar, V., Sorsa, T., Arighi, E., Weich, H., Saksela, O. & Alitalo, K. (1998) *J. Biol. Chem.* **273,** 6599–6602.
14. Mäkinen, T., Jussila, L., Veikkola, T., Karpanen, T., Kettunen, M. I., Pulkkanen, K. J., Kauppinen, R., Jackson, D. G., Kubo, H., Nishikawa, S.-I., *et al.* (2001) *Nat. Med.* **7,** 199–205.
15. Lyon, M. F. & Glenister, P. H. (1984) *Mouse News Lett.* **71,** 26.
16. Lyon, M. F. & Glenister, P. H. (1986) *Mouse News Lett.* **74,** 96.
17. Iljin, K., Karkkainen, M. J., Lawrence, E. C., Kimak, M. A., Uutela, M., Taipale, J., Pajusola, K., Alhonen, L., Halmekytö, M., Finegold, D. N., *et al.* (2001) *FASEB J.* **15,** 1028–1036.
18. Thurston, G., Suri, C., Smith, K., McClain, J., Sato, T. N., Yancopoulos, G. D. & McDonald, D. M. (1999) *Science* **286,** 2511–2514.
19. Kubo, H., Fujiwara, T., Jussila, L., Hashi, H., Ogawa, M., Shimizu, K., Awane, M., Sakai, Y., Takabayashi, A., Alitalo, K., *et al.* (2000) *Blood* **96,** 546–553.
20. Banerji, S., Ni, J., Wang, S. X., Clasper, S., Su, J., Tammi, R., Jones, M. & Jackson, D. G. (1999) *J. Cell Biol.* **144,** 789–801.
21. Weninger, W., Partanen, T. A., Breiteneder-Geleff, S., Mayer, C., Kowalski, H., Mildner, M., Pammer, J., Sturzl, M., Kerjaschki, D., Alitalo, K., *et al.* (1999) *Lab. Invest.* **79,** 243–251.
22. Joukov, V., Sorsa, T., Kumar, V., Jeltsch, M., Claesson-Welsh, L., Cao, Y., Saksela, O., Kalkkinen, N. & Alitalo, K. (1997) *EMBO J.* **16,** 3898–3911.
23. Chen, H., Chedotal, A., He, Z., Goodman, C. S. & Tessier-Lavigne, M. (1997) *Neuron* **19,** 547–559.
24. Paterna, J. C., Moccetti, T., Mura, A., Feldon, J. & Bueler, H. (2000) *Gene Ther.* **7,** 1304–1311.
25. Zolotukhin, S., Byrne, B. J., Mason, E., Zolotukhin, I., Potter, M., Chesnut, K., Summerford, C., Samulski, R. J. & Muzyczka, N. (1999) *Gene Ther.* **6,** 973–985.
26. McKendry, J. B. J., Kindsay, W. K. & Gerstein, M. C. (1957) *Pediatrics* **19,** 21–35.
27. Lee, C.-H. & Young, J. R. (1953) *J. Pediatr.* **42,** 83–86.
28. Rockson, S. G. (2001) *Am. J. Med.* **110,** 288–295.
29. Soker, S., Takashima, S., Miao, H. Q., Neufeld, G. & Klagsbrun, M. (1998) *Cell* **92,** 735–745.
30. Gluzman-Poltorak, Z., Cohen, T., Herzog, Y. & Neufeld, G. (2000) *J. Biol. Chem.* **275,** 18040–18045.
31. Mäkinen, T., Olofsson, B., Karpanen, T., Hellman, U., Soker, S., Klagsbrun, M., Eriksson, U. & Alitalo, K. (1999) *J. Biol. Chem.* **274,** 21217–21222.
32. Enholm, B., Karpanen, T., Jeltsch, M., Kubo, H., Stenback, F., Prevo, R., Jackson, D. G., Ylä-Herttuala, S. & Alitalo, K. (2001) *Circ. Res.* **88,** 623–629.
33. Hiltunen, M. O., Laitinen, M., Turunen, M., Jeltsch, M., Hartikainen, J., Rissanen, T. T., Laukkanen, J., Niemi, M., Kossila, M., Hakkinen, T. P., *et al.* (2000) *Circulation* **102,** 2262–2268.
34. Puumalainen, A. M., Vapalahti, M., Agrawal, R. S., Kossila, M., Laukkanen, J., Lehtolainen, P., Viita, H., Paljarvi, L., Vanninen, R. & Yla-Herttuala, S. (1998) *Hum. Gene Ther.* **9,** 1769–1774.
35. Monahan, P. E. & Samulski, R. J. (2000) *Mol. Med. Today* **6,** 433–440.
36. Byrne, C., Tainsky, M. & Fuchs, E. (1994) *Development* **120,** 2369–2383.
37. Robertson, S. C., Tynan, J. A. & Donoghue, D. J. (2000) *Trends Genet.* **16,** 265–271.
38. Baldwin, M. E., Catimel, B., Nice, E. C., Roufail, S., Hall, N. E., Stenvers, K. L., Karkkainen, M. J., Alitalo, K., Stacker, S. A. & Achen, M. G. (2001) *J. Biol. Chem.* **276,** 19166–19171.
39. Orlandini, M. & Oliviero, S. (2001) *J. Biol. Chem.* **276,** 6576–6581.
40. Nibbs, R. J. B., Kriehuber, E., Ponath, P. D., Parent, D., Qin, S. X., Campbell, J. D. M., Henderson, A., Kerjaschki, D., Maurer, D., Graham, G. J., *et al.* (2001) *Am. J. Pathol.* **158,** 867–877.
41. Cao, Y., Linden, P., Farnebo, J., Cao, R., Eriksson, A., Kumar, V., Qi, J.-H., Claesson-Welsh, L. & Alitalo, K. (1998) *Proc. Natl. Acad. Sci. USA* **95,** 14389–14392.
42. Plate, K. H. (2001) *Nat. Med.* **7,** 151–152.